Amine functionalized lignin-based mesoporous cellular carbons for CO_2 capture

Suleiman Sani, Xin Liu, Lee Stevens, Haomin Wang, Chenggong Sun[$]**

Faculty of Engineering, University of Nottingham, Nottingham NG7 2TU, UK

***$ Present Address**:*

School of Chemical Engineering, University of Birmingham, Birmingham, B15 2TT

****Corresponding author and email address:***

Xin Liu (xin.liu@nottingham.ac.uk)

Chenggong Sun (Cheng-gong.Sun@nottingham.ac.uk)

Abstract

Amine-impregnated mesoporous carbon sorbents have been considered one of the most promising sorbents for CO_2 capture from streams with low CO_2 concentrations. In this work, a series of novel solid amine adsorbents were prepared by impregnating polyethyleneimine (PEI) on mesoporous carbons using low-cost bio-waste material "lignin" as a carbon precursor via a facile templating method. Our results demonstrated that the mesoporous carbon with 3D interconnected porous structure and large pore size and pore volume exhibited excellent CO_2 adsorption capture of 2.90-3.13 mmol/g at a temperature operating window of 75-90 °C under CO_2 partial pressure of 0.15 bar, being significantly higher than PEI impregnated sorbents prepared by using mesoporous carbon with 2D porous structures and also many amine-impregnated carbon-based sorbents reported in previous studies. The well-developed 3D interconnected mesoporous structure, high pore volume (up to 1.80 cm^3/g), and large pore size permit the facile dispersion and immobilization of PEI within their pores and high availability of amine groups, which significantly improves both the CO_2 adsorption capacity and kinetics. In addition, the cyclic adsorption-desorption test showed that the PEI-impregnated sorbents exhibit superior thermo-stability. These results indicate that the PEI-

impregnated mesoporous adsorbents are promising ideal candidates for post-combustion CO_2 capture. This work provide a potential strategy to prepare advancved amine impregnanted mesoporous carbons from lignin for efficient carbon capture.

Keywords:

Lignin, Mesoporous carbon, Polyethylenimine, Carbon capture

1. Introduction

The increasing concentration of atmospheric carbon dioxide (CO_2) from about 277 ppm in 1750 to about 412 ppm in 2020, mainly caused by the combustion of fossil fuels like coal, petroleum, and natural gas, has raised serious concerns about the environment and ecosystem on the Earth because of its greenhouse effect [1,2]. As a result, it has attracted global political attention, with countries across the world agreeing on a plan to control the emission of CO_2 [3]. The carbon capture and storage (CCS) technique has been recognized by the Intergovernmental Panel on Climate Change as a major technology to drastically reduce CO_2 emissions [4]. At present, a wide variety of technologies such as absorption in liquids [5,6], adsorption on solids [7,8], cryogenic distillation [9], and membrane technology [10] have been proposed for the capture of CO_2 from the flue gas. Among those CCS technologies, chemical absorption using aqueous amine solutions (e.g., monoethanolamine or methyldiethanolamine), which reacts with CO_2 to produce carbamates, is the state-of-the-art technology in the industry for effective CO_2 capture [11,12]. Although amine scrubbing technology shows over 98% capture efficiency and selectivity at very low CO_2 concentration [13], several disadvantages exist, such as high corrosiveness to equipment, large capital, and operational cost, high energy consumption for solvent regeneration, thermal and oxidative degradation [14]. Therefore, the solid adsorbent-based capture process has been considered a potential alternative post-combustion carbon capture technology.

Recently, significant research interest has been focused on amine-functionalized solid adsorbents due to their advantages of high adsorption capacity and selectivity and low energy

consumption for CO_2 capture from a gas mixture. Generally, amine-functionalized solid adsorbents can be produced via chemical grafting [15,16], and physical impregnation [17-19]. Chemical grafting by forming chemical bound between the amino silanes and hydroxyl groups on the porous silica surface results in amine adsorbents with high thermal and chemical stability, however, the synthetic methods are complicated and most of the sorbents suffer from low CO_2 adsorption capacity under flue gas condition as a result of limited amine grafting level on the silica surface. In comparison, physical impregnation has been preferred from the perspective of industrial application because of its simplicity, lower cost, high amine loading level, and capability for large-scale production [20,21]. Polyethylenimine (PEI) is the most commonly used amine to prepare solid amine adsorbents [22,23]. *However, compared to chemical grafting, the physically impregnated amines including PEI suffer from degradation issues during regeneration process. Many strategies including the addition of moisture as stripping gas, functionalization of PEI molecules have been developed, which can significantly improve the thermal and oxidative stability of PEI sorbents [24, 25].*

Various porous supports especially mesoporous materials including carbon-based porous materials and mesoporous silicas [26-28] have been considered potential candidates to prepare PEI-functionalized solid adsorbents [29-37]. Mesoporous carbons are particularly attractive as support for the preparation of PEI-functionalized adsorbents. One significant advantage of mesoporous carbon supports over silica materials is their excellent thermal and electrical conductivity, making them potential candidates to be used in the electric swing adsorption (ESA) process. Being different from the conventional temperature swing adsorption process (TSA), the electrical current could be directly passed through the adsorbents to regenerate the adsorbents via “in-situ” heating by the Joule effect, which could potentially reduce the regeneration energy consumption [36,38]. Various mesoporous carbons prepared via templating methods have been employed to fabricate PEI/mesoporous carbon sorbents for CO_2 adsorption with the hard templating method using different porous materials such as zeolites, opals, and mesoporous silicas as template-leading the way because of their tunable

79 textural properties widely available carbon sources [39-41]. Previous investigations have
80 shown that mesoporous carbons with large pore volumes and controlled pore sizes are
81 preferable candidates to prepare PEI-functionalized CO_2 sorbents [33,34,42,43]. Wang et al.
82 studied the CO_2 adsorption performance of mesoporous carbons with different pore volumes
83 (0.64-2.69 cm^3/g) and pore sizes (2.2- 7.3 nm) at a PEI loading level of 50 wt% and found
84 that the adsorption capacity increased with the increase of total pore volume and pore size
85 [33]. Chen et al. synthesized a series of mesoporous carbon spheres with a controlled pore
86 size (7.6-10.8 nm) and pore volume (1.25 to 2.68 cm^3/g) via a hard template reverse emulsion
87 method [42]. It was found that the increase of pore volume and pore size could effectively
88 improve the PEI loading level and amine accessibility and therefore a high CO_2 capture
89 capacity of 3.22 mmol/g and fast adsorption rate was achieved at a partial pressure of 0.05
90 bar and temperature of 75 ^oC. A similar trend was also found by Xie et al. for PEI-modified
91 resorcinol-based mesoporous carbon aerogels [44]. Compared to pore volume, pore size
92 appears to play a critical role in determining the CO_2 diffusion and amine accessibility in
93 sorbents. Kong and Liu prepared ordered mesoporous carbon with a large pore volume of
94 3.40 cm^3/g and pore size 2.2 to 8.2 nm via self-assembly of phloroglucinol-formaldehyde and
95 triblock copolymer template (Pluronic F-123) [37]. The PEI-impregnated sorbents yielded
96 adsorption capacities of 2.58 and 1.84 mmol/g in pure CO_2 and at 30 ℃ and 75 ℃, respectively.
97 However, the adsorption capacity of PEI/mesoporous carbon sorbents was even slightly lower
98 than that of PEI-impregnated mesoporous carbon nanospheres (MCNs) with a pore size of 9
99 nm and pore volume of 0.52 cm^3/g at 75 °C and pure CO_2. By using colloidal silica as a
100 template, Wang et al. synthesized mesoporous carbon spheres (MCSs) with a large pore size
101 of 16.6 nm and pore volume of 2.87 cm^3/g, and a high CO_2 adsorption capacity of 3.71 mmol/g
102 at 15% CO_2 and 75 ^oC was achieved by PEI modified mesoporous carbon spheres [38].

103 The above brief literature review shows the great potential of mesoporous carbons as supports
104 to prepare PEI-functionalized sorbents for CO_2 adsorption. However, most mesoporous
105 carbons are synthesized via a complicated synthetic protocol and expensive and/or toxic

106 precursors including resorcinol formaldehyde were used [33,35,45-47]. Meanwhile, the pore
107 size of most mesoporous carbon, mainly determined by the template, was usually small (< 10
108 nm), which limited their application as support to preparing PEI-based sorbents for CO_2
109 adsorption. The modern industry prefers renewable materials, specifically, those obtained
110 from low-cost, abundant, environmentally benign biomass [48,49]. In this work, we reported
111 the development of PEI-functionalized solid adsorbents for highly effective CO_2 capture by
112 using mesoporous carbons derived from lignin, the third most abundant amorphous polymer
113 in nature, as support. The mesoporous carbon was prepared through a facile hard template
114 route using an abundantly low-cost bio-waste material “lignin” as carbon precursor and
115 spherical mesocellular foam (MCF) silica with 3D connected porous structure and large pore
116 size and pore volume as templates. The effects of pore structure, amount of PEI loading, and
117 capture temperature of the PEI-functionalized mesoporous carbon materials as adsorbents
118 for CO_2 adsorption were studied.

119 **2. Experimental section**

120 **2.1 Chemicals and materials**

121 Lignin (Mw = ~10,000, pH = 10.5), Tetrahydrofuran (THF), Sodium hydroxide (NaOH), and
122 Polyethylenimine (Mw = 600, branched, liquid, PEI (600b)) were all purchased from Sigma-
123 Aldrich Co. PQ mesoporous silica commercial grade was obtained from PQ Corporation.

124 **2.2 Preparation of Mesoporous Carbons and Polyethylenimine (PEI) impregnated CO_2**
125 **adsorbents**

126 The mesoporous carbons were developed through a hard templating route using mesocellular
127 foam as the templates. The mesocellular foam silica (MCF2) was prepared according to the
128 procedure reported by Sun et al. [50]. The lignin-based ordered mesoporous carbons were
129 prepared via a solvothermal method, using both the MCF silicas and the commercially
130 available mesoporous silica purchased from PQ Corporation as the hard templates. In a typical
131 synthesis, 2.4 g of lignin was dissolved in 15 mL tetrahydrofuran (THF) and added to 1.2 g of

the MCF-silicas (MCF2) with vigorous stirring until complete dissolution. Once dissolved, the mixture was heated at 50 ˚C for 24 h to allow the THF to evaporate. Then the composites were heated at different temperatures (700 ˚C, 800 ˚C, and 900 ˚C) for 1 h with a heating rate of 5 ˚C/min under Nitrogen at 1 L/min. Finally, the carbonized product was treated with a 3.0 g NaOH solution to remove the silica template. The carbon product was filtered, washed with distilled water to reach pH 7, and dried overnight in an oven at 100 ˚C. A set of samples were prepared by varying the amount of carbon precursor using MCF silica templates. This impregnation process was repeated using PQ mesoporous silica commercial grade. The MCs produced from the various MCF2 were denoted as MC2-n-m, where n represents the carbonization temperature and m is the mass ratio. In contrast, the mesoporous carbon prepared from PQ-silica was denoted MCPQ-n-m respectively. The variation in preparation conditions is shown in Table 1.

Table 1. Summary of synthesis conditions used for different ordered mesoporous carbon materials

Mesoporous carbon	Hard Template	Carbonization temperature, ˚C	Template/lignin ratio by mass
MC2-700-1	MCF2	700	1:1
MC2-800-1	MCF2	800	1:1
MC2-700-2	MCF2	700	1:2
MC2-800-2	MCF2	800	1:2
MC2-900-2	MCF2	900	1:2
MCPQ-700-1	PQ-Silica	700	1:1
MCPQ-800-1	PQ-Silica	800	1:1
MCPQ-700-2	PQ-Silica	700	1:2
MCPQ-800-2	PQ-Silica	800	1:2
MCPQ-900-2	PQ-Silica	900	1:2

147 The PEI-impregnated mesoporous carbons were prepared using a wet impregnation method
148 according to the procedure reported by Sun and co-workers [50]. In a typical preparation, a
149 calculated amount of PEI was dissolved in 10 mL of water under continuous stirring using a
150 magnetic stirrer for 10 min, after which 0.2 g of MC, or MCPQ was gradually added to the
151 solution. After overnight stirring, the resultant slurry was dried at 40 ˚C in a vacuum oven for
152 24 h to produce PEI-functionalised mesoporous carbon samples. The various PEI-
153 impregnated mesoporous carbon materials are designated as MC or MCPQ-x, where x
154 denotes the weight percentage of the PEI in the adsorbent.

155 **2.3 Characterisation of the Sorbents**

156 An ASAP 2420 (Micrometrics) apparatus was used to determine the nitrogen adsorption-
157 desorption isotherms at -196 °C. The samples were degassed before each measurement at
158 120 °C for 15 h before the analysis. The Brunauer-Emmette-Teller (BET) method was used to
159 calculate the specific surface area [51]. The total pore volume was calculated from the
160 adsorbed amount at a relative pressure, P/P_o = 0.99 using the Density Functional Theory
161 (DFT) method. The pore size distribution, pore size, and window size of the MCF-silica and
162 mesoporous carbon materials were determined according to the Barrett-Joyner-Halenda
163 method [52]. Fourier Transform Infrared (FT-IR) spectra of the samples were generated by a
164 Bruker IFS66 with a Specac "Golden Gate" ATR attachment. The FT-IR spectra were recorded
165 by accumulating 128 scans per sample at a spectral resolution of 8 cm^{-1}. Scanning Electron
166 Microscopy of the mesoporous carbon samples was carried out in a JEOL 7100F Field
167 Emission Gun Scanning Electron Microscope (FEG-SEM) (JEOL USA, Inc.). A LECO CHN-
168 2000 was used for determining the C, H, and N content of selected pristine carbon and PEI-
169 loaded carbons.

170 **2.4 CO_2 Capture Measurements of the PEI-modified Mesoporous Carbon Adsorbents**

171 The CO_2 adsorption performance of all the samples under anhydrous conditions was
172 determined using a thermogravimetric analyzer (TGA Q500 instrument), in a gas mixture

consisting of 15 % CO_2 in N_2. In a typical adsorption procedure, about 25 mg of the sample was placed in a small platinum sample pan, heated to 110 ˚C in the N_2 atmosphere at a flow rate of 100 mL $min^{-1,}$ and held at 110 ˚C for about 30 min to remove any moisture and pre-adsorbed gases. The sample was then allowed to cool down, the temperature was lowered to the adsorption temperature of 75, 80, 85, and 90 ˚C, and the gas was switched to 15 % CO_2 in N_2 at a flow rate of 100 mL min^{-1} and held for 60 min to carry out adsorption. The CO_2 adsorption capacity of the sample in mmol g^{-1} was determined from the weight gain by the sample during the adsorption process. An empty platinum pan was used as a blank correction under identical conditions. Cyclic adsorption-desorption testing was also performed. In each cyclic test, the sample was first allowed to reach adsorption temperature at 75 ˚C in the simulated flue gas (15 % CO_2/85% N_2) for 10 min for the adsorption test, and then the temperature of the sample was heated up to 110 ˚C and kept at this temperature for 10 min to desorb the adsorbed CO_2, with the gas switched to N_2. The sample temperature is then allowed to cool down to 75 ˚C to begin another cyclic test. The CO_2 adsorption/desorption test was repeated for 50 cycles.

2.5 Adsorption kinetic models

To better understand the performance of the polyethylenimine (PEI) impregnated mesoporous carbon adsorbents during the CO_2 adsorption process, the three adsorption kinetic models [53] shown in Equation 1-3 were adopted for all the samples to analyze the adsorption process.

Pseudo-first order: $q_t = q_e \cdot (1 - e^{(-K_1 \cdot x)})$ (1)

Pseudo-second order: $q_t = \frac{{q_e}^2 \cdot K_2 \cdot x}{1 + q_e \cdot K_2 \cdot x}$ (2)

Avrami: $q_t = q_e \cdot (1 - e^{-\frac{(K_a \cdot x)^n}{n}})$ (3)

Where q_t (mmol g^{-1}) and q_e (mmol g^{-1}) are the adsorption capacities of the sorbents at a given time t and equilibrium state. K_1, K_2, and K_a are the rate constant for the pseudo-first-order equation, pseudo-second-order equation, and Avrami's fraction

order model, respectively, and x is the variable that represents the time elapsed. n is Avrami's exponent.

3. Results and discussion

3.1. Pore structure of mesoporous carbons and PEI-impregnated adsorbents.

Lignin-derived mesoporous carbons with ordered 3D-interconnected porous structure and large pore size and pore volume via a facile hard-templating approach using 3D spherical mesocellular foam silica (MCF) have been proposed and successfully developed by our research group [54]. The pore volume and pore size could be regulated by varying the preparation parameters including template-to-lignin ratio and carbonization temperature. In this research, spherical mesocellular foam silica (MCF) with a large pore size of 19.0 nm, and pore volume of 3.58 cm^3/g was selected as a template and used to prepare lignin-derived mesoporous carbons. As a comparison, mesoporous carbons were also synthesized by using mesoporous silica with a 2D porous structure with a smaller pore volume of 2.79 cm^3/g but a larger pore size of 23.8 nm as a template. Both were used as support to prepare PEI-based sorbents. Figure 1 and Figure S1 show the N_2 adsorption-desorption isotherms of mesoporous carbon materials. As can be seen, all the pristine MC2 samples (Figure 1a and S1) exhibited a type IV isotherm with H2b hysteresis loop at a medium and high relative pressure (P/Po), indicating the pore networks with ink-bottle shape mesopores [55,56]. A similar hysteresis loop was observed for the mesoporous carbons prepared while the nitrogen adsorption capacity varied under different conditions. In comparison, MC2-800-1 exhibited the highest nitrogen adsorption capacity and largest hysteresis loop, indicating the highest mesopore volume achieved by MC2-800-1 among all the samples. The pore size distributions showed a bimodal mesoporous structure with peaks centered at around 4-10 nm, originating from the removal of silica walls, and 20-27 nm and the coalescence of the partially filled silica pores with the precursor when the silica walls were removed, with the mesopores centered at 20-27 nm being dominant (Figure 1b). Compared to the MC2 samples, It can be found that the N_2 adsorption-desorption isotherms of all the mesoporous carbon materials prepared using PQ silica

exhibited two obvious capillary condensation steps in the range of relative pressure of 0.45-1.0, indicating the existence of two mesopore systems (Figure 1c). Being different from MCF-derived mesoporous carbons, two types of mesopores with almost equal significance were observed, which were centered at about 4-6 nm and 19 nm, respectively. Figure 1 also shows the nitrogen adsorption isotherms of selected PEI-based sorbents. As expected, the nitrogen adsorption capacity decreased with the increasing PEI loading level from 40 to 60 wt. %, indicating that the mesopores of the adsorbents were occupied by amine molecules. A similar hysteresis loop with reduced nitrogen adsorption capacity was observed for all PEI-based sorbents, suggesting the preservation of the pristine porous structure of mesoporous carbons. As shown in Figure 1b, the intensity of all peaks reduced drastically with increasing PEI loading from 40 to 60 wt%. More importantly, both micropores and small mesopores (4-10 nm) were reduced to near zero after different levels of PEI impregnation, indicating that all those small pores were ocupied and blocked by PEI molecules.

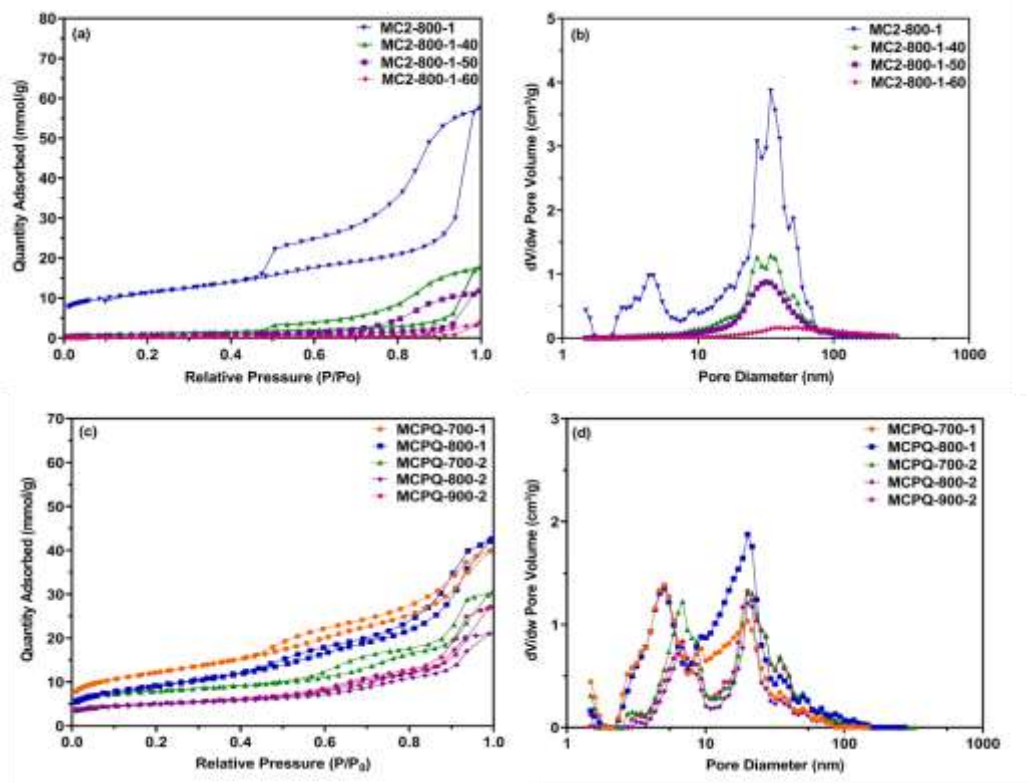

Figure. 1. Nitrogen adsorption-desorption isotherms (a), (c), and pore size distributions (b), (d) of all MC2 samples, MC2-800-1 with different PEI loadings, and MCPQ samples.

Table 2. Textural properties of mesoporous carbon support before and after PEI loadings.

Sample	S_{BET}[a] (m^2g^{-1})	V_{total}[b] (cm^3g^{-1})	$V_{meso > 10\ nm}$[c] (cm^3g^{-1})	$V_{meso\ 10\text{-}100nm}$[d] ($cm^3g^{-1}$)
MC2-700-1	735	1.12	0.23	0.72
MC2-800-1	900	1.80	0.34	1.28
MC2-800-1-40	91	0.58	0.04	0.52
MC2-800-1-50	48	0.40	0.018	0.37
MC2-800-1-60	12	0.13	0.0054	0.10
MC2-700-2	788	0.80	0.14	0.50
MC2-800-2	716	1.15	0.26	0.74
MC2-900-2	543	0.89	0.088	0.71
MCPQ-700-1	971	1.12	0.52	0.43
MCPQ-800-1	719	1.30	0.51	0.70
MCPQ-700-2	650	0.95	0.32	0.48
MCPQ-800-2	400	0.56	0.19	0.30
MCPQ-900-2	394	0.78	0.24	0.48

Note: [a] BET-specific surface area, [b] Total pore volume calculated at a relative pressure of 0.99, [c] Mesopore volume of pores smaller than 10 nm, [d] Mesopore volume of pores between 10-100 nm calculated by the DFT method.

Table 2 summarizes the textural properties of all the samples. The pristine MC2 samples possessed BET surface area in the range of 543-900 m^2g^{-1}, a total pore volume of 0.80-1.80 cm^3g^{-1}. In comparison, the BET surface area of the mesoporous carbons prepared by using mesoporous silica with a 2D porous structure is similar (394-900 m^2g^{-1}) whereas the total pore volume is much smaller than the MC2 samples prepared under similar conditions. More importantly, MCF-derived mesoporous carbons exhibit a much higher pore volume of large mesopores than the samples prepared by using mesoporous silica with a 2D porous structure as a template. The large mesopores allow a high amount of PEI loading with good dispersion, and could effectively improve the amine accessibility, and reduce the diffusion resistance of CO_2 molecules [42,43]. After PEI loading, a sharp decrease in BET surface area and mesopore volume of MC2-800-1 was observed with an increase in PEI loading level from 40 to 60 wt. %, confirming that PEI has been successfully impregnated into the mesopores of MC2-800-1. It is also notable that the adsorbent MC2-800-1-60 still had a surface area of 12

m^3/g and pore volume of 0.13 cm^3/g, indicating that there are still available porous spaces for CO_2 diffusion in the pores at such a high PEI loading level of 60 wt%.

3.2. Morphology

Figure 2 and S2 shows the SEM images of PQ silica, MC2-800-1, and the resultant adsorbents with different PEI loading levels. The morphological properties of MCF including SEM and TEM images have been shown in our previous work [54]. It can be found that the morphology of the obtained mesoporous carbons originated from the molecular geometry of the template, MCF, which is in the form of large aggregates assembled by small spheres. A high-resolution image reveals the open polygonal networks framed by carbon struts (Figure 2a-b). As shown in Figure 2c-h, the open polygonal networks could barely be seen with the increase of PEI loading level from 0 to 60 wt%, suggesting that the mesopores are gradually occupied by PEI molecules, which is inconsistent with the BET results shown in Figure 1 and Table 1. Moreover, at a low PEI loading level of 40 wt%, the sorbents showed a distinct spherical framework feature of MC2-800-1. With further increase of PEI loading level, the small particles of mesoporous carbon tend to assemble into larger particles, which is presumably due to the presence of PEI molecules on the external surface at a high amine loading level that acted as a binder for the agglomeration of small particles.

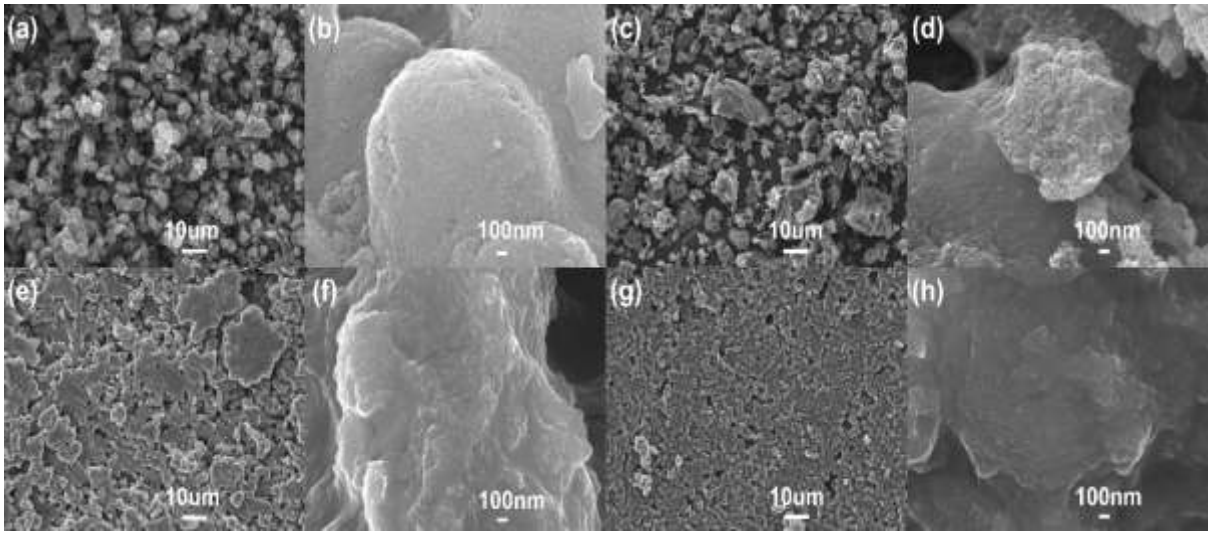

Figure. 2. Low and high magnification SEM images of MC2-800-1 (a, b), MC2-800-1-40 (c, d), MC2-800-1-50 (e, f), and MC2-800-1-60 (g, h).

3.3 Fourier Transform Infrared Spectroscopy (FT-IR) Analysis.

FT-IR spectra of selected mesoporous carbon, MC2-800-1, and its derived PEI sorbents are shown in Figure 3. It can be found that MC2-800-1 displayed a band at 800 cm^{-1} for a benzene ring [57,58]. The peak of Si-O-Si bonds at 1060 cm^{-1} was also observed in MC2-800-1 [57], suggesting that there is silica residue remaining in mesoporous carbon after NaOH washing. Further TGA test showed that the ash content of MC2-800-1 is less than 3 wt%, indicating that most of the silica has been washed out (Figure S3). After PEI impregnation, new peaks at around 1550 and 1450 cm^{-1} were observed, which correspond to the asymmetric and symmetric bending vibration peaks related to NH_2 and the N-H bending vibration in PEI [34,59]. Moreover, the C-N stretching vibration could also be found at 1250 cm^{-1} [60]. The peaks for NH_2, N-H, and C-N increased with the increase in PEI loading level. All the above results confirm that PEI/mesoporous carbons were successfully developed by the wet impregnation process.

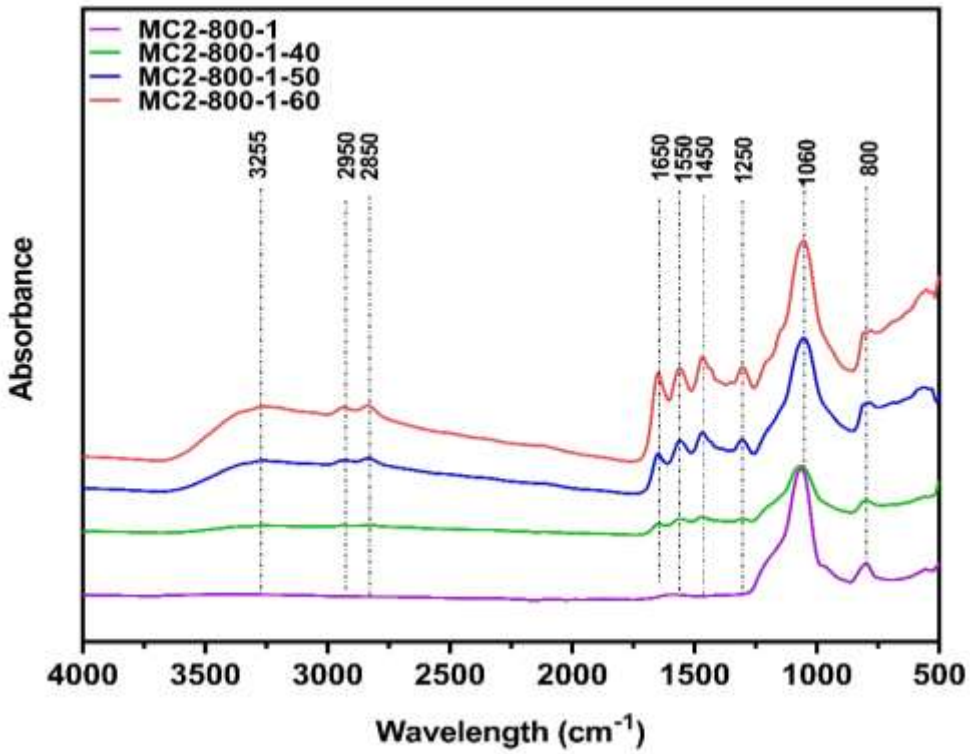

Figure. 3. FT-IR Spectra of MC2-800-1 and PEI/MC2-800-1 adsorbents.

3.4 CO_2 adsorption performance of the PEI-impregnated Mesoporous Carbon Adsorbents

The CO_2 adsorption performance of PEI/mesoporous carbon sorbents at different PEI loading levels was first evaluated at an adsorption temperature of 75 °C and CO_2 partial pressure of 0.15 bar and the results are shown in Figure 4a. It can be seen that all the PEI-modified sorbents showed increased CO_2 adsorption capacity with increasing amine loading levels while the sorption capacity varied with the textural properties of the mesoporous carbons. The PEI-modified sorbents prepared by using MC2-800-1 with the largest mesopore volume exhibited much higher adsorption capacity at different PEI loading levels between 40-60 wt% than other mesoporous carbon-based sorbents. The significantly enhanced CO_2 adsorption capacities of the PEI/mesoporous carbon adsorbents may be attributed to the strong chemical reaction between CO_2 and the amine groups [43]. Among different samples, MC2-800-1-60 with a PEI loading level of 60 wt% gave rise to the highest adsorption capacity of 129.9 mg-CO_2/g-adsorbent (2.94 mmol-CO_2/g), followed by MC2-800-1-50, MC2-900-2-60, and MC2-800-2-60, which make them have potential as ideal sorbent materials for CO_2 capture with electric swing adsorption (ESA) [38]. Table S1 shows the replicate preparation and test of the selected best-performing sorbent, MC2-800-1-60. It can be found that the standard deviation is very small, < 0.05, highlighting the high repeatability and reliability of the obtained results. As shown in Figure 4b, a linear relationship between total pore volume and CO_2 adsorption capacity at different amine loading levels was observed and the linear correlation coefficient (R^2) increased with increasing amine loading level from 0.53 to 0.81, highlighting the important role of pore volume in determining the CO_2 adsorption capacity of final carbon especially at high amine loading level, which agrees well with previous investigations [41,61]. The larger pore volume of porous support could effectively improve the surface dispersion of PEI on pore walls and hence higher CO_2 adsorption capacity can be achieved. It can also be found from Figure 4b that a relatively large deviation was observed for the sample with a small pore

volume < 1 cm^3/g, which is presumably due to the overladed PEI on the external surface of the sample.

To investigate the impact of porous structure on the performance of PEI-modified mesoporous carbon sorbents, the CO_2 adsorption performance of PEI-modified MCPQ adsorbents was also tested and the results are shown in Figure 4c and S4. Similar to PEI-modified MC sorbents, the CO_2 adsorption capacities increased with increasing PEI loading from 40 to 60 wt% while the MCPQ-based sorbents exhibited a much lower adsorption capacity. As shown in Figure S4a, CO_2 adsorption capacity at various amine loading levels increased with increasing total pore volume of the carbon materials with a linear correlation coefficient (R^2) ranged between 0.40 to 0.68. Among these adsorbents, MCPQ-800-1-60 with a PEI loading level of 60 wt% exhibits the highest capacity of only 85.6 mg-CO_2/g-adsorbent, which was about 50% lower than MC2-800-1-60. Moreover, it seems that using MC carbon support with 3D interconnected porous structures could effectively improve the accessibility of PEI into the pores, and therefore higher adsorption capacity was achieved compared to mesoporous carbons with 2D porous structures. For instance, the pore volume of MC2-900-2 was much smaller than that of MCPQ-800-1 while the adsorption capacity of MC2-900-2-60 at a PEI loading level of 60 wt% was even higher than that of MCPQ-800-1-60. The over results suggest the critical role of the 3D-interconnected porous structure by enhancing the accessible sorption sites of the sorbents. A summary of PEI-modified mesoporous carbon and silica sorbents reported by previous studies was shown in Table 3. At an operating temperature of 75 °C and high PEI loading of 60 wt.%, the adsorption capacity of MC2-800-1 is higher than some PEI-impregnated silica sorbents or most of the amine-modified mesoporous carbons reported in previous studies shown in Table 3. Meanwhile, it is also notable that the adsorption capacity of MC2-800-1-60 was higher than that of sorbents prepared by using mesoporous carbons with much larger pore volume but much smaller pore size [37,42], indicating that the large pore size could effectively improve the CO_2 adsorption capacity of PEI/mesoporous carbon sorbents.

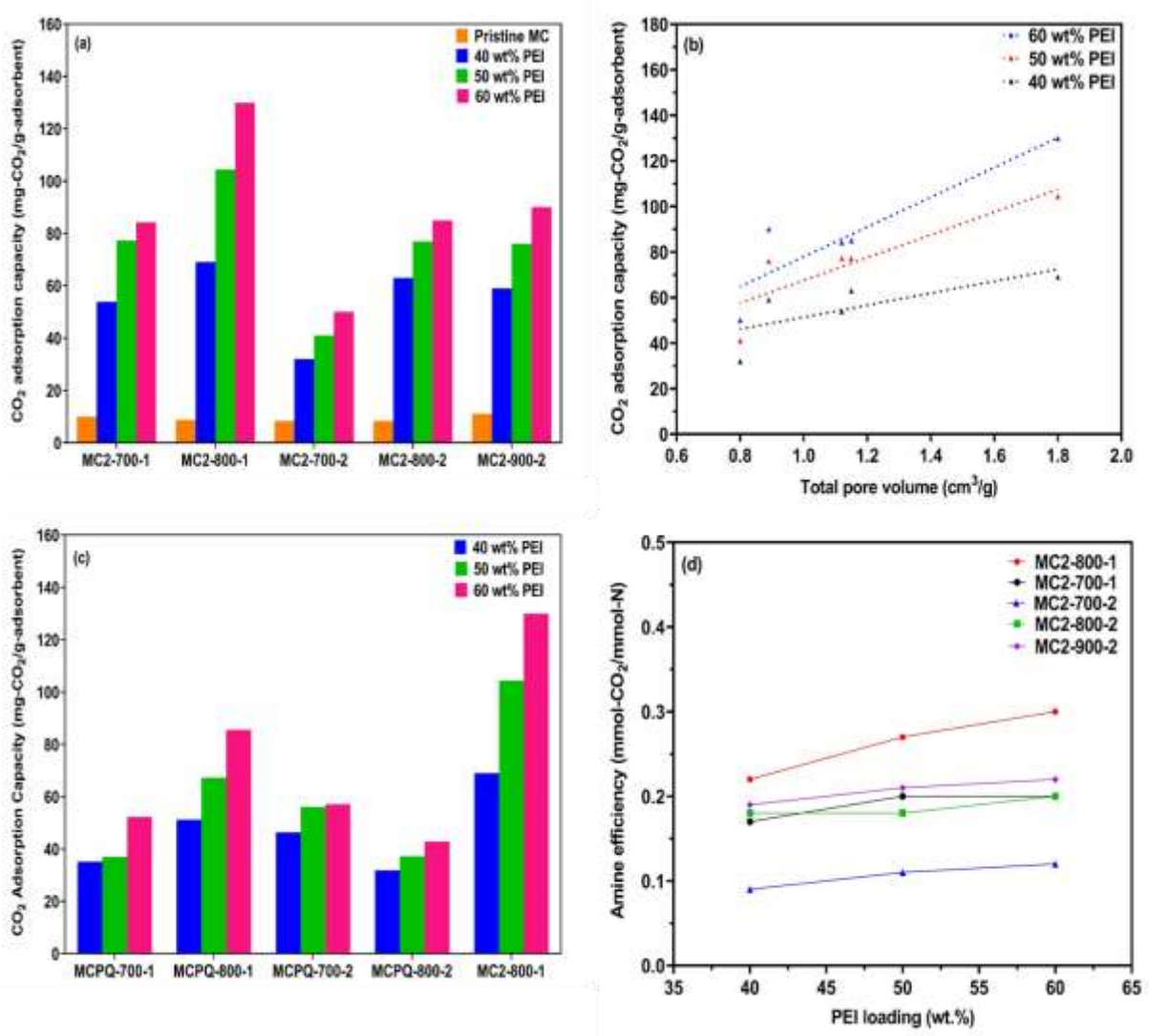

Figure. 4. CO_2 adsorption performance of mesoporous carbons and PEI-impregnated adsorbents (a), adsorption performance of PEI-impregnated MC2 adsorbents, and their relationship with the total pore volume of mesoporous carbon support (b), CO_2 adsorption performance of PEI-impregnated MCPQ adsorbents (c), and effect of PEI loadings on CO_2 amine efficiencies of mesoporous carbon adsorbents (d).

Table 3. CO_2 adsorption capacities of various amine-modified adsorbents reported in the literature and this work.

Samples	Adsorption temperature (°C)	Pressure (bar)	Adsorption capacity (mmol g^{-1})	Reference
MC2-800-1-60	75	0.15	2.95	This work
	85	0.15	3.13	
MCNs	75	1	1.97	[62]
Mesoporous carbon spheres	75	0.05	3.22	[42]
Activated ordered mesoporous carbon	75	0.15	1.84	[37]
POP	75	1	1.0	[63]
MCM-41	75	0.15	2.03	[20]
SBA-15	75	0.15	3.18	[20]
MC-PEI(65)	75	1	4.82	[34]
MCM-41	75	1	2.95	[64]
PEI-STPR-3	75	0.3	1.09	[46]
MC(PEI 50)	75	0.1	1.30	[36]
MC(TETA 43)	75	0.1	1.85	[36]
ZSM-5(PEI 33..3)	40	0.1	2.63	[65]
Meso-13X (PEI 33)	100	0.1	1.82	[66]
CA-K-1 (PEI 55)	75	0.05	2.06	[44]
CA-K-1 (PEI 60)	75	0.05	2.03	[44]
MCS-50	75	0.15	3.71	[38]
CDMC	100	1	3.72	[43]
MC-1.5-60	30	1	4.67	[47]
NOMC-L-0.5	25	1	2.50	[67]
G_900(100)	30	0.9	1.47	[68]
OMC (CMK-3)	20	1	1.7	[69]
N-OMC-750	25	0.15	1.64	[70]
OMC-20-80-24-700	25	1	2.78	[71]

According to the PEI loading level and CO_2 capacity, the amine efficiencies could be estimated as the molar ratio of CO_2 adsorbed to the amine groups, as displayed in Figure 4d. Under dry conditions, the mechanism for the reaction of amine groups with CO_2 was known that the

primary and secondary amines could react strongly with CO_2 through the formation of zwitterionic intermediates to produce carbamate salts (Eqs. 4 and 5) [72]. The formations are as follows;

$$2RNH_2 + CO_2 \leftrightarrow RNH_3 + RNHCOO \quad (4)$$

$$2R_2NH + CO_2 \leftrightarrow RNH_2 + R_2NCOO \quad (5)$$

Elemental analysis of selected samples shown in Table S2 confirmed that the actual PEI loading level is almost the same as the amount of PEI added in wet impregnation. So, the amine efficiency was calculated based on the amount of PEI added and the results are shown in Figure 4d. It can be found that the amine efficiency increased linearly with the increasing amine loading level from 40 to 60 wt.% for all the adsorbents. MC2-800-1-60 exhibited the maximum amine efficiency of 0.30 mol CO_2/mol-N with a PEI loading level of 60 wt%. It is also notable that the PEI-modified sorbents prepared by using MC2-800-1 with the largest pore volume had higher amine efficiency (0.21-0.30 mol CO_2/mol-N) than other samples with different amine loading levels. In comparison, the amine efficiency of MCPQ sorbents is much lower than MC sorbents with the maximum amine efficiency of only up to 0.20 mol CO_2/mol-N (Figure S4b). It is also notable that the amine efficiency of MC2-700-1 was higher than MCPQ-700-1 with same pore volume and MCPQ-800-1 with even higher pore volume. This suggests that the large pore size and 3D interconnected porous structure of MC carbons originated from MCF silica can effectively improve the accessibility of amine groups on the pore surface and therefore provide enhanced amine efficiency.

Figure 5 shows the CO_2 adsorption kinetics at 75 ℃ and the times taken to attain 70%, and 90% of the equilibrium adsorption capacity for the PEI/impregnated mesoporous carbon adsorbents. As seen in Figure 5a, the CO_2 adsorption on PEI-functionalized mesoporous carbon materials follows a two-stage process; a rapid CO_2 uptake within the first few minutes of adsorption, which is due to the surface chemical reaction between CO_2 and PEI [29,73]; followed a comparatively slow CO_2 adsorption process controlled by CO_2 diffusion within the

phase of supported amine. The adsorption kinetics of the PEI/impregnated mesoporous carbon adsorbents were evaluated by comparing the times taken to attain 70% (T70), and 90% (T90) of the equilibrium adsorption capacity for the PEI/impregnated mesoporous carbon adsorbents, as exhibited in Figure 5 (c and e). Generally, it can be seen that the 70% (T70), and 90% (T90) varied with both mesoporous carbon supports and PEI loading amount for impregnation. The PEI-modified sorbents prepared by using MC2-800-1 with the largest pore volume exhibited the fastest adsorption rate with a much shorter time being required to achieve 70% and 90% of the equilibrium adsorption capacity than other samples. In comparison, PEI-modified sorbents prepared with MC2-700-2, which had the smallest pore volume, showed the longest T70, and T90, suggesting that the low adsorption rate originated from the greatly increased thickness or reduced CO_2 accessibility of the amine layer on pore walls as a result of the small pore volume. The CO_2 adsorption on the PEI-functionalized mesoporous carbons with 2D porous structures follows a similar two-stage process, as shown in Figure 5b. In comparison, the CO_2 adsorption of MC carbons was overall much faster than MCPQ carbons. For instance, the T70, and T90 of MC2-800-1-60 were just 1.35 and 7.81 min, respectively, which is 2 and 3 times faster than the 2.9 and 22.9 min achieved for the best MCPQ sorbent, MCPQ-800-1-60. Although the pore volume of MC2-700-1 was smaller than that of MCPQ-800-1, the T70, and T90 of MC2-700-1-60 were shorter than that of MCPQ-800-1-60. The above results suggest that the 3D interconnected porous structure of MC carbons could potentially facilitate greater accessibility of amines and reduced CO_2 diffusion resistance, leading to a faster CO_2 adsorption rate as well as higher CO_2 adsorption capacity.

To further evaluate the CO_2 adsorption kinetics on both PEI impregnated MC and MCPQ carbons, pseudo-first-order model, pseudo-second-order model, and Avrami model were applied to fit the at 75 °C and 15 % CO_2. The CO_2 adsorption capacity and all the kinetic fitting parameters are listed in Table 4. It can be seen that Avrami's fraction-order model can better describe the CO_2 adsorption process on polyethylenimine (PEI) impregnated mesoporous carbon adsorbents as the correlation coefficients of Avrami's fraction-order model is higher

than pseudo-second-order model and pseudo-first-order model. This suggests that the CO2 adsorption on PEI impregnated MC and MCPQ carbons follows a multiple adsorption pathway, involving both physical and chemical adsorption [75]. As shown in Table 4, the rate constant (k_a), an indicator of adsorption rate, decreased with increasing amine loading level, which is attributable to the reduced accessibility of CO_2 into the porous matrix after amine impregnation [74]. In comparison, the rate constant of PEI impregnated MCPQ carbons was much lower than PEI impregnated MC carbons. Amongst all samples, PEI impregnated MC2-800-2 exhibited the highest adsorption rate, highlighting the critical role of pore interconnectivity, pore size and pore volume in determining the CO_2 adsorpotive properties of amine modified mesoporous carbons.

Table 4. Adsorption kinetic results for PEI impregnated sorbents

Sample	Pseudo-first order			Pseudo-second order			Avrami's fraction-order			
	q_e	K_1	R^2	q_e	K_2E3	R^2	q_e	K_a	n	R^2
MC2-700-1-40	51.01	0.9636	0.6990	52.72	0.0300	0.9204	54.03	0.0469	0.3485	0.9585
MC2-700-1-50	71.85	0.7544	0.6236	74.93	0.0156	0.8741	80.90	0.0110	0.3048	0.9604
MC2-700-1-60	78.83	0.7848	0.7120	82.10	0.0149	0.9111	85.11	0.0347	0.3528	0.9408
MC2-800-1-40	67.02	1.2900	0.9186	68.56	0.0346	0.9184	66.92	1.6090	1.3000	0.9229
MC2-800-1-50	100.60	0.9580	0.9039	103.70	0.0161	0.9194	100.40	1.1900	1.2920	0.9075
MC2-800-1-60	124.70	0.7742	0.9037	129.20	0.0102	0.9224	124.40	0.9575	1.2730	0.9064
MC2-700-2-40	29.80	0.4981	0.7160	31.29	0.0272	0.9292	32.70	0.0271	0.3626	0.9887
MC2-700-2-50	37.65	0.2315	0.7599	40.78	0.0093	0.9252	47.32	0.0064	0.3585	0.9969
MC2-700-2-60	45.59	0.1643	0.8003	50.42	0.0051	0.9303	65.21	0.0027	0.3611	0.9983
MC2-800-2-40	59.18	0.7838	0.6566	61.54	0.0205	0.8956	64.60	0.0227	0.3282	0.9611
MC2-800-2-50	70.77	0.4715	0.6437	74.75	0.0102	0.8784	83.82	0.0067	0.3144	0.9673
MC2-800-2-60	77.89	0.4567	0.5869	82.32	0.0090	0.8467	99.93	0.0014	0.2734	0.9769
MC2-900-2-40	55.63	0.8696	0.6935	57.67	0.0245	0.9161	59.40	0.0401	0.3484	0.9583
MC2-900-2-50	70.40	0.6861	0.6220	73.56	0.0147	0.8747	79.77	0.0103	0.3068	0.9651
MC2-900-2-60	82.67	0.6343	0.5951	86.80	0.0110	0.8501	98.91	0.0038	0.2850	0.9555
MCPQ-700-1-40	32.85	0.4137	0.7458	34.70	0.0204	0.9382	36.22	0.0286	0.3816	0.9876
MCPQ-700-1-50	33.97	0.1964	0.7782	37.10	0.0086	0.9270	44.50	0.0048	0.3619	0.9971
MCPQ-700-1-60	47.17	0.2160	0.6914	51.29	0.0069	0.8808	76.91	0.0004	0.2920	0.9855
MCPQ-800-1-40	49.38	1.0282	0.7822	50.79	0.0363	0.9667	50.81	0.1346	0.4115	0.9692
MCPQ-800-1-50	63.31	0.7097	0.6995	65.93	0.0178	0.9204	68.22	0.0356	0.3554	0.9676
MCPQ-800-1-60	79.08	0.6025	0.6716	83.08	0.0111	0.8900	89.49	0.0143	0.3309	0.9491
MCPQ-700-2-40	43.16	0.5775	0.6216	45.22	0.0210	0.8787	49.70	0.0076	0.3023	0.9839
MCPQ-700-2-50	52.91	0.5082	0.6494	55.69	0.0148	0.8872	61.34	0.0086	0.3165	0.9748
MCPQ-700-2-60	52.91	0.5052	0.6545	55.71	0.0147	0.8894	61.15	0.0094	0.3200	0.9736
MCPQ-800-2-40	29.58	0.4056	0.6706	31.31	0.0216	0.8964	35.02	0.0071	0.3212	0.9875
MCPQ-800-2-50	34.02	0.3080	0.6779	36.39	0.0141	0.8908	43.69	0.0029	0.3110	0.9903
MCPQ-800-2-60	12.59	0.0872	0.9410	14.98	0.0070	0.9790	17.14	0.0109	0.5269	0.9997

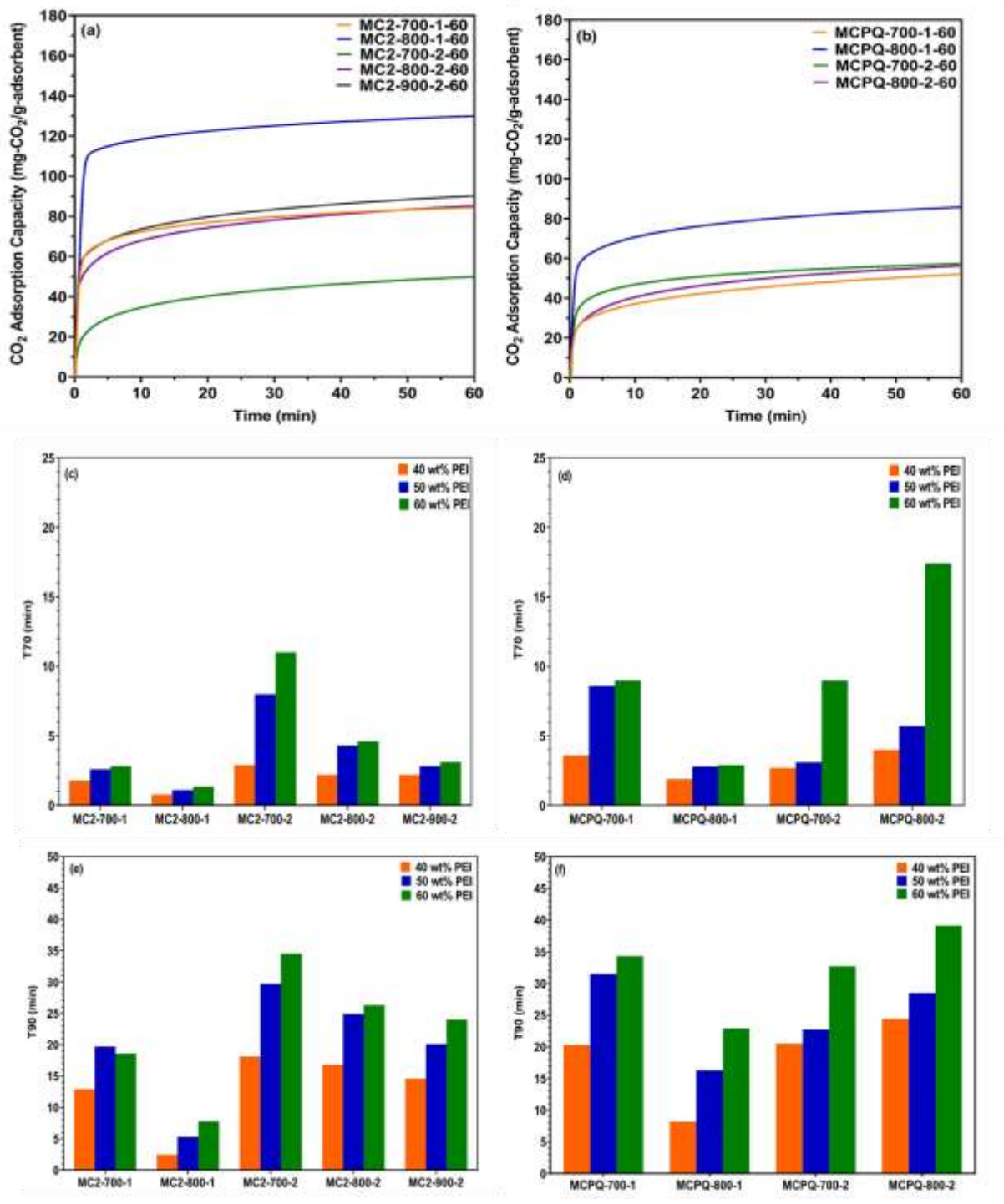

Figure. 5. CO_2 adsorption kinetics profiles at 75 ℃ and 15% CO_2 in N_2 and, the time taken to achieve 70% and 90% of the equilibrium adsorption capacity of PEI-impregnated mesoporous carbon adsorbents (a,c,e), and PEI-impregnated MCPQ adsorbents (b,d,f).

The pseudo-first-order model, pseudo-second-order model, and Avrami model were applied to evaluate the adsorption kinetics of polyethylenimine (PEI) impregnated mesoporous carbon adsorbents at 75 °C and 15 % CO_2. The CO_2 adsorption capacity and its corresponding fitting curves are shown in Figure S5, and all the kinetic fitting parameters are listed in Table 4.

3.5 Effect of temperature on CO_2 adsorption performance.

To examine the variation of CO_2 adsorption capacity of the best-performing PEI-modified sorbent, MC2-800-1-60, along with the adsorption temperature, the adsorption performance of MC2-800-1-60 at a temperature range between 75-90 °C was tested and the results are shown in Figure 6. It can be seen that the adsorption capacity of MC2-800-1-60 first increased and then decreased with adsorption temperature, with the highest adsorption capacity of 137.7 mg-CO_2/g-adsorbent (3.13 mmol/g) being achieved at an adsorption temperature of about 85 °C. Overall, MC2-800-1-60 showed a high CO_2 adsorption capacity of 2.90-3.13 mmol/g in the temperature range between 75-90 °C, highlighting the relatively wide operating window of MC2-800-1-60 and the potential for reduction of energy required to cool down the flue gas. Figure 6b shows the time taken to reach 70% (T70), 80% (T80), and 90% (T90) of equilibrium CO_2 adsorption capacity for MC2-800-1-60 at different adsorption temperatures. It was found that adsorption temperature also had a significant impact on the CO_2 adsorption rate of MC2-800-1-60. T90 was sharply reduced with the increase in adsorption temperature. For instance, T90 was only about 4 min at an adsorption temperature of 90 °C, which was only half of the T_{90} achieved at an adsorption temperature of 75 °C. This indicates that high adsorption temperature could help to overcome the kinetic barrier of CO_2 adsorption by improving the mobility and accessibility of impregnated PEI molecules and reducing the diffusive resistance of CO_2.

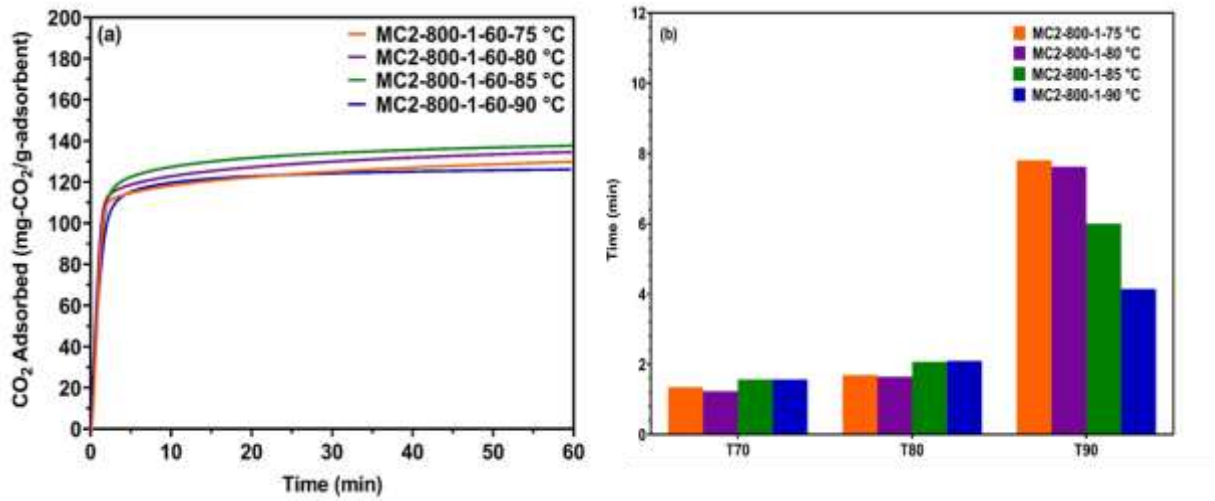

Figure 6. Effect of temperature on CO_2 adsorption capacity (a) and adsorption kinetics (b) of MC2-800-1-60 at 15% CO_2 in N_2.

3.6 Cyclic stability test of PEI-impregnated mesoporous carbon.

In addition to high CO_2 adsorption capacity and fast adsorption rate, the good cyclic stability of solid adsorbents throughout adsorption-desorption cycles are also critical from a practical point of view. Therefore, MC2-800-1-60 as the best-performing PEI-impregnated adsorbent was selected for a cyclic adsorption-desorption experiment under simulated flue gas conditions by using the temperature swing method. As shown in Figure 7, a slight decrease of only 5.42% in CO_2 adsorption capacity from 129 mg/g to 122 mg/g was observed after 50 consecutive adsorption-desorption cycles, which is presumably due to the evaporation loss of PEI molecules with lower molecular weight present in PEI that has been reported in previous studies [30, 75]. This result confirms the highly cyclic stability of PEI-modified mesoporous carbons for long-term operation under temperature swing adsorption process. Moreover, considering the high thermal conductivity of carbon based materials, carbon sorbents can be potentially regenerated via in-situ heating, 'Joule effect', by introducing electricity into the system. It has been reported in the previous study [38] that the PEI modified mesoporous carbons could be rapidly heated up under electrical current and the adsorbed CO_2 could be quickly released within 30 min. Carbon based sorbents that can be directly regenerated by

renewable electricity in stead of heat from fossil fuels represent a promising sorbent for carbon capture.

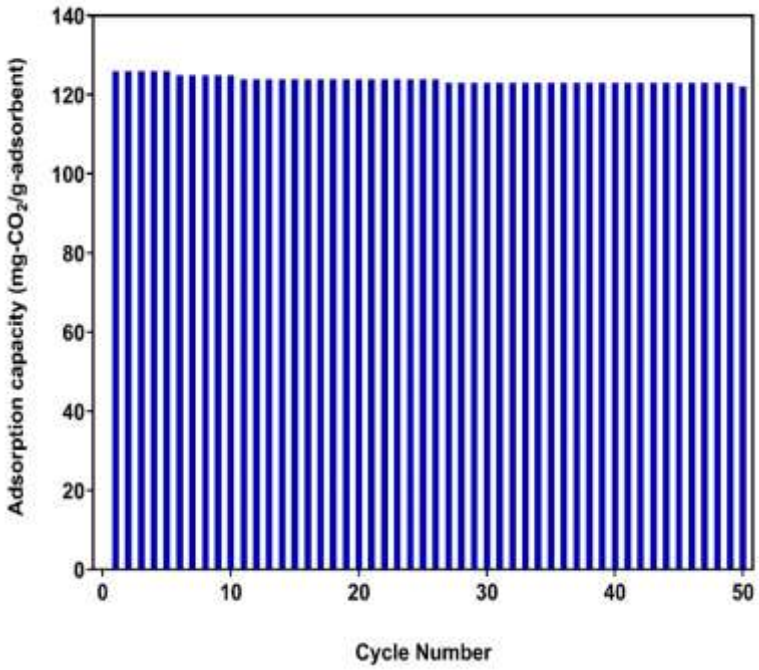

Figure 7. Cyclic adsorption-desorption profiles of MC2-800-1-60 in simulated flue gas with a CO_2 partial pressure of 0.15 bar in N_2. Conditions: adsorption temperature; 75 °C; desorption temperature: 110 °C.

4. Conclusions

In summary, we developed a series of polyethyleneimine (PEI)-functionalized sorbents for CO_2 capture in which mesoporous carbon materials with 3D interconnected pore structures solid supports prepared from green precursor lignin provided higher pore volumes and pore sizes. The characterizations carried out in this study demonstrate that PEI-functionalized mesoporous carbon adsorbents exhibit high CO_2 adsorption capacity, fast adsorption kinetics, high amine efficiency, and good regeneration performance. At the optimal PEI loading of 60 wt%, the CO_2 adsorption capacity of the best-performing PEI mesoporous carbon adsorbent (MC2-800-1) was found to be 129 mg-CO_2/g-adsorbent (2.95 mmol/g) at 75 °C, and 137.7 mg-CO_2/g-adsorbent (3.13 mmol/g) at 85 °C in the simulated flue gas of 15% CO_2 in N_2, which is 52% higher than those of the PEI-functionalized MCPQ with 2D pore networks Furthermore, PEI functionalized mesoporous carbon sorbents showed very good regenerability and stability

of CO_2 adsorption under temperature swing adsorption process, where the adsorption capacity decreased by less than 6% after 50 adsorption cycles. The findings in our work conclude that the lignin-derived mesoporous carbon adsorbents have a good potential as a promising alternative to aqueous amines for large-scale CO_2 capture from industries. Moreover, the high thermal conductivity of carbon based materials unlocks the possibilities to directly use electricity or renewable electricity for the regeneration of sorbents, which requires future efforts to develop an electric swing adsorption process for carbon based sorbents.

Acknowledgments

The authors wish to acknowledge the Nigeria Government for funding Suleiman Sani's Ph.D. research through the Petroleum Technology Development Fund (PTDF) Overseas Scholarship Scheme (OSS) (PTDF/ED/PHD/SS/1293/17). The authors also thank Mr. Nigel Neate for carrying out the FEG-SEM imaging measurements.

References

[1] Cox PM, Betts RA, Jones CD, Spall SA, Totterdell IJ. Acceleration of global warming due to carbon-cycle feedbacks in a coupled climate model. Nature. 2000;408(6809):184-7.

[2] Friedlingstein P, Jones MW, O'Sullivan M, Andrew RM, Bakker DC, Hauck J, Le Quéré C, Peters GP, Peters W, Pongratz J, Sitch S. Global carbon budget 2021. Earth Syst. Sci. Data, 2022, 14(4), 1917-2005.

[3] Mac Dowell N, Fennell PS, Shah N, Maitland GC. The role of CO_2 capture and utilization in mitigating climate change. Nat. Clim. Change. 2017;7(4):243-9.

[4] Metz B, Davidson O, De Coninck HC, Loos M, Meyer L. IPCC special report on carbon dioxide capture and storage. Cambridge: Cambridge University Press; 2005.

[5] Bishnoi S, Rochelle GT. Absorption of carbon dioxide into aqueous piperazine: reaction kinetics, mass transfer and solubility. Chem. Eng. Sci. 2000;55(22):5531-43.

[6] Agbonghae EO, Hughes KJ, Ingham DB, Ma L, Pourkashanian M. Optimal process design of commercial-scale amine-based CO_2 capture plants. Ind. Eng. Chem. Res.. 2014;53(38):14815-29.

[7] Inui T, Okugawa Y, Yasuda M. Relationship between properties of various zeolites and their carbon dioxide adsorption behaviors in pressure swing adsorption operation. Ind. Eng. Chem. Res. 1988;27(7):1103-9.

[8] Trickett CA, Helal A, Al-Maythalony BA, Yamani ZH, Cordova KE, Yaghi OM. The chemistry of metal–organic frameworks for CO_2 capture, regeneration and conversion. Nature Reviews Materials. 2017;2(8):1-6.

[9] Font-Palma C, Cann D, Udemu C. Review of cryogenic carbon capture innovations and their potential applications. C. 2021;7(3):58.

[10] Brunetti A, Scura F, Barbieri G, Drioli E. Membrane technologies for CO_2 separation. J. Membr. Sci. 2010;359(1-2):115-25

[11] Figueroa JD, Fout T, Plasynski S, McIlvried H, Srivastava RD. Advances in CO_2 capture technology—the US Department of Energy's Carbon Sequestration ProgramInt. J. Greenh. Gas Control. 2008;2(1):9-20.

[12] Yang H, Xu Z, Fan M, Gupta R, Slimane RB, Bland AE, Wright I. Progress in carbon dioxide separation and capture: A review. J. Environ. Sci. Stud. 2008 ;20(1):14-27.

[13] Rochelle GT. Amine scrubbing for CO_2 capture. Science. 2009;325(5948):1652-4.

[14] Oschatz M, Antonietti M. A search for selectivity to enable CO_2 capture with porous adsorbents. Energy Environ. Sci. 2018;11(1):57-70.

[15] Bezerra DP, da Silva FW, de Moura PA, Sousa AG, Vieira RS, Rodriguez-Castellon E, Azevedo DC. CO_2 adsorption in amine-grafted zeolite 13X. Appl. Surf. Sci. 2014;314:314-21.

[16] Hou X, Zhuang L, Ma B, Chen S, He H, Yin F. Silanol-rich platelet silica modified with branched amine for efficient CO_2 capture. Chem. Eng. Sci. 2018;181:315-25.

[17] Drage TC, Arenillas A, Smith KM, Snape CE. Thermal stability of polyethylenimine based carbon dioxide adsorbents and its influence on selection of regeneration strategies. Microporous Mesoporous Mater. 2008;116(1-3):504-12.

[18] Jung H, Lee CH, Jeon S, Jo DH, Huh J, Kim SH. Effect of amine double-functionalization on CO_2 adsorption behaviors of silica gel-supported adsorbents. Adsorption. 2016;22(8):1137-46.

[19] Meng Y, Jiang J, Gao Y, Aihemaiti A, Ju T, Xu Y, Liu N. Biogas upgrading to methane: Application of a regenerable polyethyleneimine-impregnated polymeric resin (NKA-9) via CO_2 sorption. J. Chem. Eng. 2019;361:294-303.

[20] Ma X, Wang X, Song C. “Molecular basket” sorbents for separation of CO_2 and H_2S from various gas streams. J. Am. Chem. Soc. 2009 ;131(16):5777-83.

[21] Zhang H, Goeppert A, Olah GA, Prakash GS. Remarkable effect of moisture on the CO_2 adsorption of nano-silica supported linear and branched polyethylenimine. J. CO_2 Util. 2017;19:91-9.

[22] Zhao J, Simeon F, Wang Y, Luo G, Hatton TA. Polyethylenimine-impregnated siliceous mesocellular foam particles as high-capacity CO_2 adsorbents. RSC Advances. 2012;2(16):6509-19.

[23] Subagyono DJ, Liang Z, Knowles GP, Chaffee AL. Amine modified mesocellular siliceous foam (MCF) as a sorbent for CO_2. Chem. Eng. Res. Des. 2011;89(9):1647-57.

[24] Zhang W, Liu H, Sun C, Drage TC, Snape CE. Performance of polyethyleneimine–silica adsorbent for post-combustion CO_2 capture in a bubbling fluidized bed. Chem. Eng. J. 2014, 251: 293-303.

570 [25] Min K, Choi W, Kim C, Choi M. Oxidation-stable amine-containing adsorbents for carbon
571 dioxide capture. Nat. commu. 2018, 9(1): 726.

572 [26] Maroto-Valer MM, Lu Z, Zhang Y, Tang Z. Sorbents for CO_2 capture from high carbon fly
573 ashes. Waste Management. 2008;28(11):2320-8.

574 [27] Wang D, Sentorun-Shalaby C, Ma X, Song C. High-capacity and low-cost carbon-based
575 “molecular basket” sorbent for CO_2 capture from flue gas. Energ Fuel. 2011;25(1):456-8.

576 [28] Liu X, Sun Y, Liu J, Sun C, Liu H, Xue Q, Smith E, Snape C. Potassium and zeolitic structure
577 modified ultra-microporous adsorbent materials from a renewable feedstock with favorable
578 surface chemistry for CO_2 capture. ACS Appl. Mater. Interfaces. 2017;9(32):26826-39.

579 [29] Liu X, Zhou K, Farndon M, Meier E, Stevens L, Liu H, Sun C. Mesocellular silica foam
580 supported polyamine adsorbents for dry CO_2 scrubbing: Performance of single versus
581 blended polyamines for impregnation. Appl. Energy. 2019;255:113643.

582 [30] Heydari-Gorji A, Belmabkhout Y, Sayari A. Polyethylenimine-impregnated mesoporous
583 silica: effect of amine loading and surface alkyl chains on CO_2 adsorption. Langmuir.
584 2011;27(20):12411-6.

585 [31] Alkhabbaz MA, Khunsupat R, Jones CW. Guanidinylated poly (allylamine) supported on
586 mesoporous silica for CO_2 capture from flue gas. Fuel. 2014;121:79-85.

587 [32] Tang Z, Han Z, Yang G, Yang J. Polyethylenimine loaded nanoporous carbon with ultra-
588 large pore volume for CO_2 capture. Appl. Surf. Sci. 2013;277:47-52.

589 [33] Wang D, Ma X, Sentorun-Shalaby C, Song C. Development of carbon-based “molecular
590 basket” sorbent for CO_2 capture. Ind. Eng. Chem. Res. 2012;51(7):3048-57.

591 [34] Wang J, Chen H, Zhou H, Liu X, Qiao W, Long D, Ling L. Carbon dioxide capture using
592 polyethylenimine-loaded mesoporous carbons. J. Environ. Sci. Stud. 2013;25(1):124-32.

[35] Wang J, Huang H, Wang M, Yao L, Qiao W, Long D, Ling L. Direct capture of low-concentration CO_2 on mesoporous carbon-supported solid amine adsorbents at ambient temperature. Ind. Eng. Chem. Res. 2015 ;54(19):5319-27.

[36] Gibson JA, Gromov AV, Brandani S, Campbell EE. The effect of pore structure on the CO2 adsorption efficiency of polyamine impregnated porous carbons. Microporous and Mesoporous Mater. 2015;208:129-39.

[37] Kong W, Liu J. Ordered mesoporous carbon with enhanced porosity to support organic amines: efficient nanocomposites for the selective capture of CO_2. New J Chem. 2019;43(15):6040-7.

[38] Wang M, Yao L, Wang J, Zhang Z, Qiao W, Long D, Ling L. Adsorption and regeneration study of polyethylenimine-impregnated millimeter-sized mesoporous carbon spheres for post-combustion CO_2 capture. Appl. Energy. 2016;168:282-90.

[39] Cho HS, Ryoo R. Synthesis of ordered mesoporous MFI zeolite using CMK carbon templates. Microporous and Mesoporous Mater. 2012;151:107-12.

[40] Park DH, Lakhi KS, Ramadass K, Kim MK, Talapaneni SN, Joseph S, Ravon U, Al-Bahily K, Vinu A. Energy efficient synthesis of ordered mesoporous carbon nitrides with a high nitrogen content and enhanced CO_2 capture capacity. Eur J Chem. 2017;23(45):10753-7.

[41] Lakhi KS, Cha WS, Choy JH, Al-Ejji M, Abdullah AM, Al-Enizi AM, Vinu A. Synthesis of mesoporous carbons with controlled morphology and pore diameters from SBA-15 prepared through the microwave-assisted process and their CO_2 adsorption capacity. Microporous and Mesoporous Mater. 2016;233:44-52.

[42] Chen Q, Wang S, Rout KR, Chen D. Development of polyethylenimine (PEI)-impregnated mesoporous carbon spheres for low-concentration CO_2 capture. Catal. Today. 2021;369:69-76.

617 [43] Peng HL, Zhang JB, Zhang JY, Zhong FY, Wu PK, Huang K, Fan JP, Liu F. Chitosan-
618 derived mesoporous carbon with ultrahigh pore volume for amine impregnation and highly
619 efficient CO_2 capture. J. Chem. Eng. 2019;359:1159-65.

620 [44] Xie W, Yu M, Wang R. CO_2 capture behaviors of amine-modified resorcinol-based carbon
621 aerogels adsorbents. Aerosol Air Qual. Res. 2017;17(11):2715-25.

622 [45] Gadipelli S, Patel HA, Guo Z. An ultrahigh pore volume drives up the amine stability and
623 cyclic CO_2 capacity of a solid-amine@ carbon sorbent. Adv. Mater. 2015;27(33):4903-9.

624 [46] Tang Z, Han Z, Yang G, Yang J. Polyethylenimine loaded nanoporous carbon with ultra-
625 large pore volume for CO_2 capture. Appl. Surf. Sci. 2013;277:47-52.

626 [47] Wang J, Wang M, Zhao B, Qiao W, Long D, Ling L. Mesoporous carbon-supported solid
627 amine sorbents for low-temperature carbon dioxide capture. Ind. Eng. Chem. Res.
628 2013;52(15):5437-44.

629 [48] Titirici MM, Antonietti M. Chemistry and materials options of sustainable carbon materials
630 made by hydrothermal carbonization. Chem. Soc. Rev. 2010;39(1):103-16.

631 [49] Titirici MM, White RJ, Brun N, Budarin VL, Su DS, del Monte F, Clark JH, MacLachlan MJ.
632 Sustainable carbon materials. Chem. Soc. Rev. 2015;44(1):250-90.

633 [50] Sun Y, Liu X, Sun C, Al-Sarraf W, Foo KZ, Meng Y, Lee S, Wang W, Liu H. Synthesis and
634 functionalisation of spherical meso-, hybrid meso/macro-and macro-porous cellular silica
635 foam materials with regulated pore sizes for CO_2 capture. J. Mater. Chem.
636 2018;6(46):23587-601.

637 [51] Sing KS. Reporting physisorption data for gas/solid systems with special reference to the
638 determination of surface area and porosity (Recommendations 1984). Pure Appl. Chem.
639 1985;57(4):603-19.

640 [52] Brunauer S, Emmett, PH, Teller, E. Adsorption of Gases in Multimolecular Layers. J. Amer.
641 Chem. Soc. 1938; 60(2): 309-19.

[53] Tiwari D, Bhunia H, Bajpai PK. Development of chemically activated N-enriched carbon adsorbents from urea-formaldehyde resin for CO_2 adsorption: Kinetics, isotherm, and thermodynamics, J. Environ. Manag. 2018;218: 579–592.

[54] Sani S, Liu, X., Li M, Stevens L, Sun C. Synthesis and characterization of three-dimensional interconnected large-pore mesoporous cellular lignin carbon materials and their potential for CO_2 capture. Microporous and Mesoporous Materials. 2023; 243:112334.

[55] Donohue MD, Aranovich GL. A new classification of isotherms for Gibbs adsorption of gases on solids. Fluid Ph. Equilibria. 1999;158:557-63.

[56] Saikia D, Wang TH, Chou CJ, Fang J, Tsai LD, Kao HM. A comparative study of ordered mesoporous carbons with different pore structures as anode materials for lithium-ion batteries. RSC Adv. 2015;5(53):42922-30.

[57] Nabavinia M, Kanjilal B, Fujinuma N, Mugweru A, Noshadi I. Developing Eco-Friendly and Cost-Effective Porous Adsorbent for Carbon Dioxide Capture. Molecules. 2021;26(7):1962.

[58] Klinthong W, Huang CH, Tan CS. One-pot synthesis and pelletizing of polyethylenimine-containing mesoporous silica powders for CO_2 capture. Ind. Eng. Chem. Res. 2016;55(22):6481-91.

[59] Wang X, Schwartz V, Clark JC, Ma X, Overbury SH, Xu X, Song C. Infrared study of CO_2 sorption over “molecular basket” sorbent consisting of polyethylenimine-modified mesoporous molecular sieve. . Phys. Chem. C. 2009;113(17):7260-8.

[60] Faisal M, Pamungkas AZ, Krisnandi YK. Study of Amine functionalized mesoporous carbon as CO_2 storage materials. Processes. 2021;9(3):456.

[61] Montiel-Centeno K, Barrera D, Villarroel-Rocha J, Moreno MS, Sapag K. Hierarchical nanostructured carbons as CO_2 adsorbents. Adsorption. 2019;25(7):1287-97.

665 [62] Chai SH, Liu ZM, Huang K, Tan S, Dai S. Amine functionalization of microsized and
666 nanosized mesoporous carbons for carbon dioxide capture. Ind. Eng. Chem. Res.
667 2016;55(27):7355-61.

668 [63] Mane S, Gao ZY, Li YX, Liu XQ, Sun LB. Rational fabrication of polyethylenimine-linked
669 microbeads for selective CO_2 capture. Ind. Eng. Chem. Res. 2018;57(1):250-8.

670 [64] Panek R, Wdowin M, Franus W, Czarna D, Stevens LA, Deng H, Liu J, Sun C, Liu H, Snape
671 CE. Fly ash-derived MCM-41 as a low-cost silica support for polyethyleneimine in post-
672 combustion CO2 capture. J. CO_2 Util.. 2017;22:81-90.

673 [65] Lee CH, Hyeon DH, Jung H, Chung W, Jo DH, Shin DK, Kim SH. Effects of pore structure
674 and PEI impregnation on carbon dioxide adsorption by ZSM-5 zeolites. J. Ind. Eng. Chem.
675 2015;23:251-6.

676 [66] Chen C, Kim SS, Cho WS, Ahn WS. Polyethylenimine-incorporated zeolite 13X with
677 mesoporosity for post-combustion CO_2 capture. Appl. Surf. Sci.. 2015;332:167-71.

678 [67] Wan X, Li Y, Xiao H, Pan Y, Liu J. Hydrothermal synthesis of nitrogen-doped ordered
679 mesoporous carbon: via lysine-assisted self-assembly for efficient CO_2 capture, RSC Adv.
680 2020;10:2932-2941.

681 [68] Maruccia E, Lourenco MAO, Priamushko T, Bartoli M, Bocchini S, Pirri FC, Saracco G,
682 Kleitz F, Gerbaldi C. Nanocast nitrogen-containing ordered mesoporous carbons from
683 glucosamine for selective CO_2 capture. Mater. Today Sustain. 2022;17:100089.

684 [69] Vorokhta M, Moravkova J, Dopita M, Zhigunov A, Slouf M, Pilar R, Sazama P. Effect of
685 micropores on CO_2 capture in ordered mesoporous CMK-3 carbon at atmospheric
686 pressure, Adsorption. 2021.

687 [70] Liu X, Zhou Y, Wang CL, Liu Y, Tao DJ. Solvent-free self-assembly synthesis of N-doped
688 ordered mesoporous carbons as effective and bifunctional materials for CO_2 capture and
689 oxygen reduction reaction, Chem. Eng. J. 2022;427:130878.

690 [71] Zhang Z, Sun N, Wei, W. Facile and controllable synthesis of ordered mesoporous carbons
691 with tunable single-crystal morphology for CO_2 capture, Carbon N. Y. 2020;161: 629-638.

692 [72] Fujiki J, Yogo K. Carbon dioxide adsorption onto polyethylenimine-functionalized porous
693 chitosan beads. Energ fuels. 2014;28(10):6467-74.

694 [73] Niu M, Yang H, Zhang X, Wang Y, Tang A. Amine-impregnated mesoporous silica
695 nanotube as an emerging nanocomposite for CO_2 capture. ACS Appl Mater Interfaces.
696 2016;8(27):17312-20.

697 [74] Liu Q, Shi J, Zheng S, Tao M, He Y, Shi Y. Kinetics studies of CO_2 adsorption/ desorption
698 on amine-functionalized multiwalled carbon nanotubes, Ind. Eng. Chem. Res. 2014;53(29):
699 11677–11683.

700 [75] Wang D, Wang X, Song C. Comparative Study of Molecular Basket Sorbents Consisting of
701 Polyallylamine and Polyethylenimine Functionalized SBA-15 for CO_2 Capture from Flue
702 Gas. ChemPhysChem, 2016;18(22): 3163-73.